The Theoretical Minimum Induced Drag of Three-Surface Airplanes in Trim

Eric R. Kendall*
Gates Learjet Corporation, Wichita, Kansas

Using the theories and theorems of Prandtl and Munk it is shown that "ideal" minimum induced drag can be achieved with a modern "three-surface" airplane in trim if equal and opposite vertical loads are applied by the forward and aft trimming surfaces. The minimum induced-drag trim condition can be attained at any center-of-gravity (c.g.) location because the two individual trim surface loads can be any size and sign as long as their sum is zero. This result is shown to be entirely consistent with the less favorable results for conventional and canard "two-surface" airplanes derived by others from the same theoretical basis. These types require zero trim surface load for minimum induced drag. This can be attained at only one aft c.g. location on a tail-aft design, and cannot be attained on a canard which requires a further forward c.g. location for inherent positive static longitudinal stability. The nonoptimum surface loadings required for trim and stability over a finite c.g. range on two-surface airplanes are reviewed. It is shown that each type incurs an induced-drag penalty that is related to the trim surface load. This penalty is significantly higher on the canard two-surface airplane due to the much larger surface loading required for trim.

Nomenclature

AR	= aspect ratio, $= b^2/S$
b	= span, ft
C_{D_i}	= induced-drag coefficient
C_L	= lift coefficient, $= W/qS_1$
D_i	= induced drag, lb
g	= intersurface gap, ft
ℓ	= longitudinal location, ft
L	= surface load, lb
M	= pitching moment, lb-ft
M_0	= wing-body zero-lift moment, lb-ft
q	= dynamic pressure, lb/ft^2
R	= Naylor's induced-drag factor
S	= surface area, ft^2
W	= airplane weight, lb
μ	= small/large span ratio
σ	= mutual drag factor

Subscripts

mn	= mth and nth surfaces
m,n	= surfaces m and n, respectively
w	= center of gravity
1,2,3	= main, tail, and forward surfaces, respectively
12	= main and tail surfaces
13	= main and forward surfaces
23	= tail and forward surfaces

I. Introduction

THEORIES developed by Prandtl[1,2] and Munk[3,4] for determining the drag of multiplanes have been used effectively by Naylor[5] and Laitone[6-8] to determine the trimming surface load required for minimum induced drag of "two-surface" airplanes such as the conventional wing-tail configuration and the less prevalent canard-wing configuration. Their analyses have shown that for practical arrangements of both types the induced drag resulting from the use of zero trim surface load is equal to or very close to the minimum attainable value.

The desired minimum induced-drag trim condition requires an aft center-of-gravity (c.g.) location and conflicts with requirements for positive static stability. A tail volume can be found to stabilize the conventional aft-tail configuration, but the canard configuration cannot attain the minimum induced drag with positive static stability. Practical canards require a large upward trim surface load for longitudinal trim. Larrabee,[9] using Prandtl's induced-drag equation for biplanes, demonstrates clearly the somewhat unexpected result that upload on the canard surface results in trimmed drag penalties of the same magnitude as those due to an equal download on the tail of a conventional wing-tail configuration. Since it is known that canard uploads are generally much higher than conventional tail downloads, Larrabee's result helps to explain the results of McLaughlin[10] and Keith and Selberg,[11] who found that canard configurations had lower flight efficiencies than conventional tail-aft designs when each type was trimmed in pitch and had similar static margins.

Potential fuel savings for a typical subsonic transport airplane with an aft tail have been estimated by Laitone[12] to be about 5% when the reduction in induced and compressibility drag are both considered. This is consistent with the trimmed drag data presented by Shevell.[13] However, it is clear that a two-surface airplane cannot maintain a trimmed condition with zero tail load over a normal operational range of c.g. locations, lift coefficients, and Mach numbers. Thus, the best that can be done with only two surfaces is to design for minimum induced drag at some "average" operational flight condition and to accept penalties for the off-design conditions.

In this paper, the Prandtl-Munk theories are used to determine the surface loading conditions that produce minimum induced drag on a modern "three-surface" configuration, such as the Gates-Piaggio GP-180 shown in Fig. 1.

This type of airplane has a wing, an aft-mounted tail, and a separate "third" surface mounted ahead of the main wing. It is shown that when both the forward and aft surfaces are used for longitudinal trim, the minimum induced-drag condition can be attained at any c.g. location. Consequently, there is no conflict between the requirements for minimum

Received Aug. 21, 1984; presented as Paper 84-2164 at the AIAA 2nd Applied Aerodynamics Conference, Seattle, WA, Aug. 21-23, 1984; revision received May 17, 1985.

*Chief, Aerodynamics and Propulsion. Associate Fellow AIAA.

drag, longitudinal trim, and positive static longitudinal stability. Thus, potential fuel savings relative to conventional and canard types are attainable in all cruise flight conditions.

Section II briefly describes the difficulties with "two-surface" designs already reported by others and mentioned previously. Then, the "three-surface" analysis, which leads to the conclusions just mentioned, is presented in Sec. III. Finally, Sec. IV outlines some practical considerations related to the theoretical results being reported.

II. Two-Surface Configurations

The principal interactions between induced drag, longitudinal trim, and static longitudinal stability for two-surface configurations are outlined briefly. The purpose is to provide a perspective for the three-surface analysis presented in Sec. III.

Minimum Induced Drag

Prandtl[1] gives the ratio of surface lift forces for minimum induced drag of elliptically loaded biplane wings as

$$\frac{L_2}{L_1}=\frac{\mu-\sigma}{(1/\mu)-\sigma}, \quad \sigma\leq\mu\leq 1 \tag{1}$$

Munk[3] showed that the total induced drag of any lifting system remains unchanged if the lifting elements are displaced relative to each other in the direction of flight as long as their lift forces remain unchanged. Thus, Eq. (1) may be used for conventional tail-aft monoplanes and canard monoplane configurations. The lift ratio L_2/L_1 is then the ratio of the trim surface lift to the wing lift, as well as the span ratio $\mu\ll 1$.

For the case of zero gap, $\mu=\sigma$ and Eq. (1) give $L_2=0$. Also, for a finite gap, $\mu>\sigma$ so $L_2>0$. These results have been obtained by Naylor[5] and Laitone[6,7] as well.

For a conventional or canard two-surface airplane, in which $\mu=0.3$ and the gap is 10% of the wing span, $\sigma=0.236$ (see Ref. 7, Table 1) and Eq. (1) gives $L_2/L_1=0.021$. Thus, the ideal lift on the trimming surface of a two-surface airplane having typical proportions is zero and slightly positive if a gap is present. However, Laitone shows that the incremental drag penalty resulting from the use of zero trim surface load when a small upload is required is negligible. Thus, the sufficiently accurate practical conclusion is that zero trim surface load produces minimum induced drag on typically proportioned two-surface airplanes.

Longitudinal Trim

The requirement to design a two-surface airplane with zero trim surface load restricts the center of gravity to only one location, as shown below. The sign convention of Fig. 2 is used to define surface loads and locations.

For balance about the wing-body aerodynamic center, the following equation applies for a conventional tail-aft design when $n=2$ and for a canard design when $n=3$

$$M_1=M_0-W(\ell_1-\ell_w)-L_n(\ell_n-\ell_1)=0 \tag{2}$$

Then, when the trim surface load is zero $L_n=0$, and

$$\ell_w-\ell_1=-M_0/W \tag{3}$$

Since M_0 is negative for most practical configurations, the center of gravity must be aft of the wing-body aerodynamic center, i.e., $\ell_w>\ell_1$. The airplane balance condition is then simply one, where the lift/weight couple balances the zero-lift moment as shown in Fig. 3.

Static Longitudinal Stability

The ability of two-surface designs to attain the ideal minimum induced drag and to have positive static longitudinal stability is reviewed below.

The moment about the airplane c.g. for either a tail-aft design ($n=2$) or a canard configuration ($n=3$) is

$$M_w=M_0-L_1(\ell_1-\ell_w)-L_n(\ell_n-\ell_w) \tag{4}$$

Differentiating with respect to angle of attack gives the following inequality for positive static longitudinal stability:

$$\frac{\partial M_w}{\partial\alpha}=-\frac{\partial L_1}{\partial\alpha}(\ell_1-\ell_w)-\frac{\partial L_n}{\partial\alpha}(\ell_n-\ell_w)<0 \tag{5}$$

Then the trim surface stabilizing moment must be such that

$$\frac{\partial L_n}{\partial\alpha}(\ell_n-\ell_w)>\frac{\partial L_1}{\partial\alpha}(\ell_w-\ell_1) \tag{6}$$

Substituting from Eq. (3) for the zero trim surface load condition gives

$$\frac{\partial L_n}{\partial\alpha}(\ell_n-\ell_w)>\frac{\partial L_1}{\partial\alpha}\left(-\frac{M_0}{W}\right) \tag{7}$$

For practical configurations M_0 is negative. Then the condition for positive static stability from Eq. (7) with $\partial L_n/\partial\alpha$ and $\partial L_1/\partial\alpha$ both positive is

$$(\ell_n-\ell_w)>0 \tag{8}$$

This requires the trimming surface to be located aft of the center of gravity, which is a condition that cannot be met by a canard design.

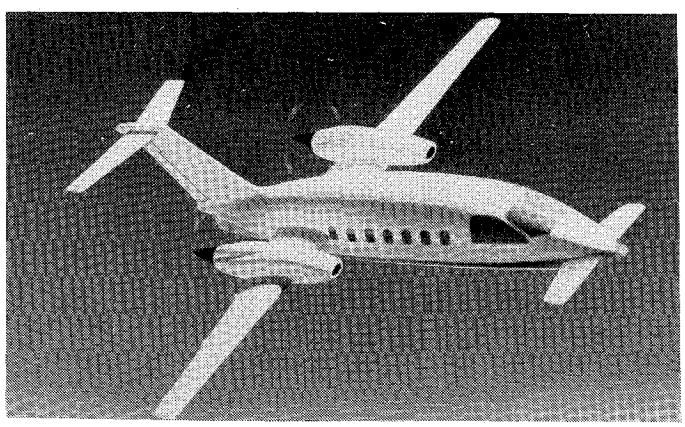

Fig. 1 Gates-Piaggio GP-180 (the Avanti).

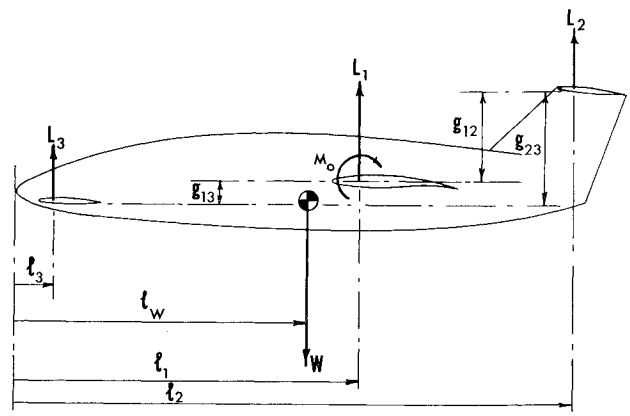

Fig. 2 System of forces and moments.

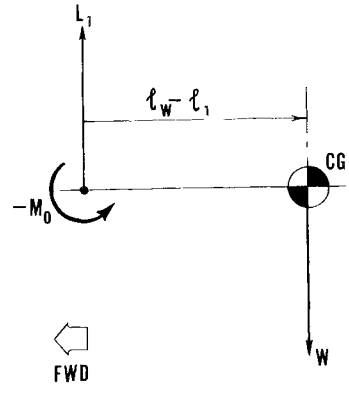

Fig. 3 Point c.g. trim with zero tail load.

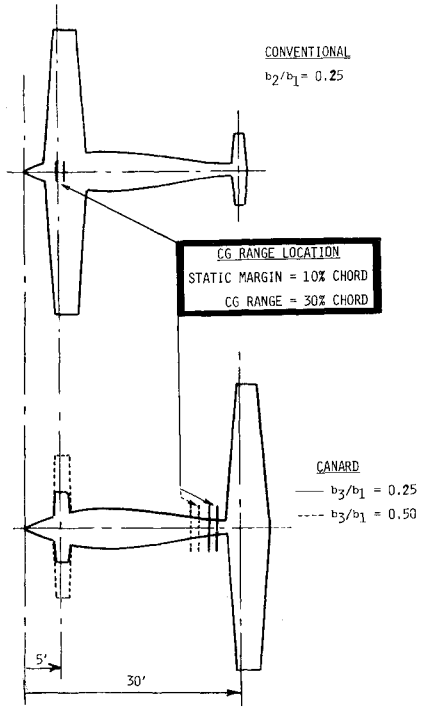

Fig. 4 Conventional and canard configurations.

Induced-Drag Penalties

The induced drag will be higher than the minimum value when the trim surface load varies significantly from the desired value of zero. This will occur when it is necessary to trim the two-surface airplane at c.g. locations other than the optimum.

Using Prandtl's[2] equation for the induced drag of a biplane, Naylor[5] derived the following expression for the ratio of actual/ideal induced drag with zero gap:

$$R = 1 + \frac{L_n^2}{(L_1 + L_n)^2}\left(\frac{b_1^2}{b_n^2} - 1\right) \tag{9}$$

Since the total lift, $L_1 + L_n$, must support the airplane's weight, W, and since b_1/b_n is a configurational constant, Eq. (9) may be written as

$$R = 1 + K(L_n/W)^2 \tag{10}$$

Clearly, an induced-drag penalty is present for positive or negative values of the trim surface load L_n.

Equation (2) gives the surface load required for trim as

$$L_n = \frac{M_0 - W(\ell_1 - \ell_w)}{\ell_n - \ell_1} \tag{11}$$

For forward c.g. locations $\ell_1 - \ell_w$ is positive and the negative weight moment, $-W(\ell_1 - \ell_w)$, adds to the usually negative wing-body zero-lift moment, M_0. Since $\ell_1 - \ell_w$ is usually much larger for positive stability of canard configurations, the trim surface load L_n and the induced-drag penalty given by Eq. (10) are usually significantly greater.

Numerical Example

The interaction between induced drag, longitudinal trim requirements, and static longitudinal stability requirements for two-surface airplanes can be seen from the following numerical example.

Figure 4 shows a conventional and canard layout, each having a trim surface/wing span ratio of 0.25.

These two airplanes also have the same wing area, trim surface area, surface spacing, total weight, and wing-body zero-lift moment. A modified canard with twice the trim surface span, area, and aspect ratio is also shown. Complete quantitative data for each airplane, including the estimated surface lifting effectiveness values for a given flight condition, are presented in Table 1.

Using these data the c.g. locations that produce a 10% minimum static margin and a 30% c.g. range are estimated for each configuration. Then, the "in-trim" trimming surface loads are computed using Eq. (11) and the actual/ideal induced-drag ratio is found from Eq. (9).

The results obtained are summarized in Table 2.

Static Stability

To produce the same minimum static margin, the aft c.g. locations relative to the wing-body aerodynamic center are:

1) Conventional	1.168 ft behind
2) Canard ($b_3/b_1 = 0.25$)	2.780 ft ahead
3) Canard ($b_3/b_1 = 0.50$)	5.250 ft ahead

It is seen that the canard designs must have aft c.g. locations that are further from the wing-body aerodynamic center than that for the conventional design.

Table 1 Data for conventional vs canard comparison

Geometric data:	
Wing area, S_w, ft^2	160
Wing span, b_w, ft	40
Wing aspect ratio, $\mathcal{R}_w$	10
Trim surface area, S_T, ft^2	17(34)
Trim surface span, b_T, ft	10(20)
Trim surface aspect ratio, $\mathcal{R}_T$	6(12)
Fuselage length, ℓ_F, ft	30
Reference chord, C, ft	4
Flight conditions:	
Aircraft weight, W, lb	12,000
Aircraft speed, V, equivalent airspeed, knots	300
Trim/stability data:	
Wing-body zero-lift moment, M_0, lb-ft	−20,000
Static margin, % chord	10
c.g. range, % chord	30
Aero assumptions:	
Lift curve slope	$2\pi\mathcal{R}/(\mathcal{R}+2)$
$1 - \partial\epsilon/\partial\alpha$	Conventional, 0.7 Canard, 1.1
Aero results:	
$\partial L_1/\partial\alpha$, lb/rad	$81{,}554\pi$
$\partial L_2/\partial\alpha$, lb/rad	$5{,}459\pi$
$\partial L_3/\partial\alpha$, lb/rad	$8{,}578\pi$ $(19{,}606\pi)$

Note: Data in parentheses are for the modified canard configuration with $b_3/b_1 = 0.5$.

Forward c.g. Location

To produce the same minimum static margin and the same usable c.g. range, the forward c.g. locations relative to the wing-body aerodynamic center are:

1) Conventional	0.032 ft ahead
2) Canard ($b_3/b_1 = 0.25$)	3.980 ft ahead
3) Canard ($b_3/b_1 = 0.50$)	6.450 ft ahead

These are all 1.2 ft further forward than the aft c.g. locations. Since the canard c.g. locations are always much further ahead of the wing-body aerodynamic center, the nose-down gravitational moment will add to the usually nose-down M_0 to produce a requirement for a large nose-up trimming moment from the canard surface.

Trim Surface Loads

The trim surface loads required to balance the airplanes are highest for each configuration at the forward c.g. limit. They are:

1) Conventional	815 lb (download)
2) Canard ($b_3/b_1 = 0.25$)	2710 lb (upload)
3) Canard ($b_3/b_1 = 0.50$)	3896 lb (upload)

It is seen that the canard surface loads for trim at forward c.g. are between 3.3 and 4.8 times higher than the magnitude of trim load required by the conventional configuration. Table 2 also shows the effect on the trim surface average pressure loading, lift coefficient, and ratio of load to wing load.

Actual/Ideal Induced-Drag Ratio

The induced-drag penalty associated with the higher trim surface loading shows up in the actual/ideal induced-drag ratio which varies with c.g. location. The results at forward c.g. are:

1) Conventional	1.069
2) Canard ($b_3/b_1 = 0.25$)	1.765
3) Canard ($b_3/b_1 = 0.50$)	1.316

Significantly higher values for the canard designs are apparent. Even though the term $[(b_1/b_3)^2 - 1]$ in Eq. (9) was reduced from a value of 15 to a value of 3 by doubling the canard span, the induced-drag penalty was only lowered from 76.5 to 31.6% of the ideal minimum induced drag. This is because the increased canard area caused a forward shift of the c.g. range for stability which, in turn, required an increased surface load for trim.

Drag/Trim/Stability Interaction

The numerical example has demonstrated the interaction between drag, trim, and stability for the two types of two-surface airplanes considered. However, due to its relative simplicity, the example may not be representative of a performance comparison between two separate optimized designs. Although the designer of a two-surface canard configuration is clearly at a disadvantage in the areas of drag, trim, and stability, there may be compensating advantages in the areas of structural weight or handling characteristics that are not addressed by this paper.

III. Three-Surface Configurations

The surface loading conditions that produce minimum induced drag on a modern "three-surface" configuration are first derived from Prandtl's drag equations. The interactions with longitudinal trim and static longitudinal stability requirements are then reviewed.

Minimum Induced Drag

Prandtl[1] reported that, "The total [induced] drag [of a multiplane] consists of the sum of all the separate drags and of as many mutual drags as there are combinations of the wings in twos." Thus, the familiar "two-surface" induced-drag equation from Ref. 2 given by

$$\pi q D_i = \frac{L_1^2}{b_1^2} + 2\sigma \frac{L_1 L_2}{b_1 b_2} + \frac{L_2^2}{b_2^2} \tag{12}$$

may be extended for three surfaces as follows:

$$\pi q D_i = \frac{L_1^2}{b_1^2} + 2\sigma_{12}\frac{L_1 L_2}{b_1 b_2} + \frac{L_2^2}{b_2^2} + 2\sigma_{23}\frac{L_2 L_3}{b_2 b_3} + \frac{L_3^2}{b_3^2} + 2\sigma_{13}\frac{L_1 L_3}{b_1 b_3} \tag{13}$$

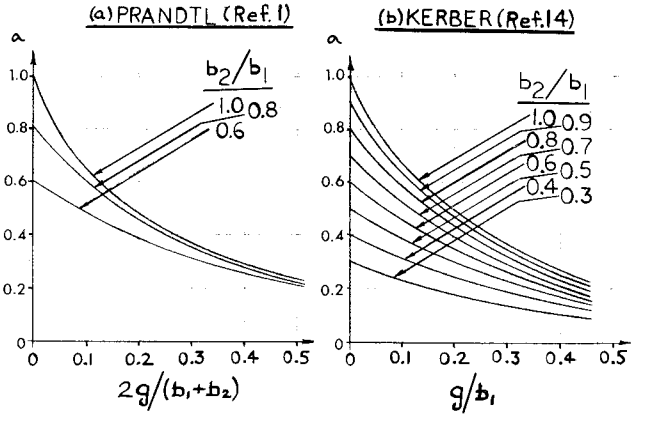

Fig. 5 Mutual drag factors.

Table 2 Results of conventional vs canard comparison

Two-surface airplane configuration	Conventional tail-aft		Pure canard			
Minimum static margin, % chord	10		10			
Center-of-gravity range, % chord	30		30			
Trim surface span/wing span	0.25		0.25		0.50[a]	
c.g. limit	Aft	Fwd	Aft	Fwd	Aft	Fwd
c.g. distance from wing-body aerodynamic center, ft	−1.168	+0.032	+2.780	+3.980	+5.250	+6.450
In-trim trimming surface load, lb	−239	−815	+2134	+2710	+3320	+3896
Trim surface loading, lb/ft^2	−14.1	−47.9	+125.5	+159.4	+97.6	+114.6
Trim surface lift coefficient	−0.046	−0.157	+0.410	+0.521	+0.319	+0.375
Ratio of trim surface load/wing load	−0.0195	−0.0636	+0.2163	+0.2913	+0.3825	+0.4808
Actual/ideal induced-drag ratio	1.006	1.069	1.474	1.765	1.229	1.316

[a]No change in trim surface chord. Both trim surface area and trim surface aspect ratio are doubled.

where the double subscripts on the mutual drag factor σ are used to identify each of the mutually interfering surface pairs.

The mutual drag factor is presented by Prandtl in Ref. 1 and by Kerber in Ref. 14. Their results are presented in Figs. 5a and 5b, respectively.

It is seen that if surface m has a longer span than surface n, then

$$\sigma_{mn} = F(b_m, b_n, g_{mn}) \leq b_n/b_m \leq 1 = b_n/b_m \text{ when } g_{mn} = 0$$

For a constant total lift, $L_1 + L_2 + L_3 = W$, the main surface lift, L_1 in Eq. (13), may be replaced by

$$L_1 = W - (L_2 + L_3) \tag{14}$$

Then,

$$\pi q D_i = \frac{W^2}{b_1^2} + \frac{(L_2+L_3)^2}{b_1^2}\left[1 - \frac{2\sigma_{12}}{b_2/b_1} + \frac{b_1^2}{b_2^2}\right] - \frac{2W(L_2+L_3)}{b_1^2}\left[1 - \frac{\sigma_{12}}{b_2/b_1}\right] + \frac{2L_1L_3}{b_1^2}\left[\frac{\sigma_{13}}{b_3/b_1} - \frac{\sigma_{12}}{b_2/b_1}\right]^{\dagger} - \frac{2L_2L_3}{b_1^2}\left[\frac{b_1^2}{b_2^2}\left(1 - \frac{\sigma_{23}}{b_3/b_2}\right)\right] + \frac{L_3^2}{b_1^2}\left[\frac{b_1^2}{b_3^2} - \frac{b_1^2}{b_2^2}\right] \tag{15}$$

If $L_2 = L_3 = 0$, $\pi q D_i = W^2/b_1^2$ or $C_{D_i} = C_L^2/\pi \mathcal{R}_1$ which is the ideal minimum induced drag for the elliptically loaded main surface. The second and subsequent terms in Eq. (15) then represent the change from the ideal minimum induced drag due to trimming loads L_2 and L_3. It is seen that the induced-drag modification due to the trimming surface loads is a function of the span ratios and mutual drag factors of all of the surface pairs.

Munk's[3] stagger theorem permits longitudinal relocation of any or all of the surfaces with no change of induced drag as long as the surface load remains unchanged. Therefore, Eq. (13) with Prandtl's mutual drag factor may be applied to a modern (highly staggered) three-surface airplane with elliptically loaded surfaces. It also permits the study of gap effects to be made without consideration of the longitudinal location of the surfaces relative to each other. It is seen from Fig. 6 that if one gap, say, g_{12}, is chosen to be zero, the resulting equation will apply to six different configurations. Munk's theorem allows the third surface to be ahead of surface 1, longitudinally between surfaces 1 and 2, or behind surface 2, with no change in total induced drag. Also, the mutual drag factor σ_{12} will be the same whether surface 3 is above or below the other two.

It follows that only three gap combinations need to be specified; namely, 1) No gaps zero. 2) One gap zero (which results in the other two gaps being identical). 3) All gaps zero. Each of these gap conditions will be considered.

No Gaps Zero

This is the most general case for which Eq. (15) applies as written. It is seen that if $L_3 = 0$, the equation reduces to

$$\pi q D_i = \frac{W^2}{b_1^2} + \frac{L_2^2}{b_1^2}\left[1 - \frac{2\sigma_{12}}{b_2/b_1} + \frac{b_1^2}{b_2^2}\right] - \frac{2WL_2}{b_1^2}\left[1 - \frac{\sigma_{12}}{b_2/b_1}\right] \tag{16}$$

This is the same as the two-surface equation obtained by Laitone [Ref. 7, Eq. (3)].

†The substituted variable L_1 is retained to simplify the grouping of the gap and span ratio terms.

For typical designs, the third surface load L_3 will be positive and its value for trim can be minimized by applying a down-load on the tail (negative L_2). If $L_2 + L_3 = 0$, Eq. (15) reduces to

$$\pi q D_i = \frac{W^2}{b_1^2} + \frac{2L_1L_3}{b_1^2}\left[\frac{\sigma_{13}}{b_3/b_1} - \frac{\sigma_{12}}{b_2/b_1}\right] - \frac{2L_2L_3}{b_1^2}\left[\frac{b_1^2}{b_2^2}\left(1 - \frac{\sigma_{23}}{b_3/b_2}\right)\right] + \frac{L_3^2}{b_1^2}\left[\frac{b_1^2}{b_3^2} - \frac{b_1^2}{b_2^2}\right] \tag{17}$$

The last term will be zero if $b_3 = b_2$; the third term will be zero with $g_{23} = 0$ and $b_3 \leq b_2$; and the second term will be zero if both of these conditions are met. Clearly, by choosing the correct gaps, span ratios and L_2/L_3 loading ratio, the induced drag can be held close to the ideal minimum value of $W^2/\pi q b_1^2$. This is demonstrated by consideration of the other gap combinations.

One Gap Zero

If $g_{23} = 0$, then $g_{12} = g_{13}$ and $\sigma_{23}/(b_3/b_2) = 1$ with $b_3 \leq b_2$. Equation (15) then becomes

$$\pi q D_i = \frac{W^2}{b_1^2} + \frac{(L_2+L_3)^2}{b_1^2}\left[1 - \frac{2\sigma_{12}}{b_2/b_1} + \frac{b_1^2}{b_2^2}\right] - \frac{2W(L_2+L_3)}{b_1^2}\left[1 - \frac{\sigma_{12}}{b_2/b_1}\right] + \frac{2L_1L_3}{b_1^2}\left[\frac{\sigma_{13}}{b_3/b_1} - \frac{\sigma_{12}}{b_2/b_1}\right] + \frac{L_3^2}{b_1^2}\left[\frac{b_1^2}{b_3^2} - \frac{b_1^2}{b_2^2}\right] \tag{18}$$

Now, if the trimming surface spans are made the same, $b_3 = b_2$. Also, because $g_{12} = g_{13}$, σ_{13} will be equal to σ_{12} and Eq. (18) becomes

$$\pi q D_i = \frac{W^2}{b_1^2} + \frac{(L_2+L_3)^2}{b_1^2}\left[1 - \frac{2\sigma_{12}}{b_2/b_1} + \frac{b_1^2}{b_2^2}\right] - \frac{2W(L_2+L_3)}{b_1^2}\left[1 - \frac{\sigma_{12}}{b_2/b_1}\right] \tag{19}$$

This is similar to Laitone's two-surface equation with $L_2 + L_3$ taking the place of the tail load L_2. Therefore, directly from Laitone's Eq. (4), the condition for minimum induced drag may be written as

$$\frac{L_2+L_3}{W} = \left[1 - \frac{\sigma_{12}}{b_2/b_1}\right] \Big/ \left\{\left[1 - \frac{2\sigma_{12}}{b_2/b_1} + \frac{b_1^2}{b_2^2}\right]\right\} \tag{20}$$

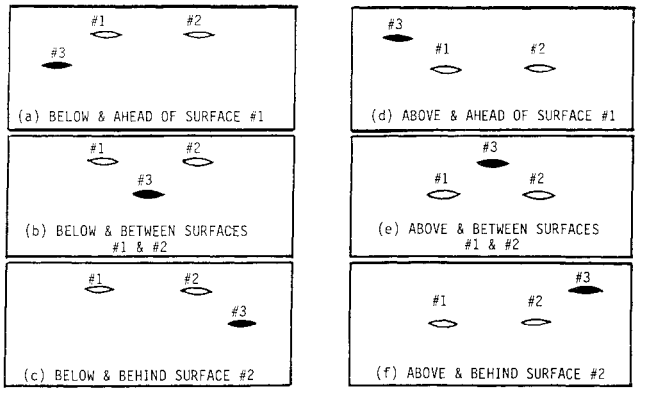

Fig. 6 Gap configurations.

Thus, the total trim surface load L_2+L_3 must be slightly positive for minimum induced drag. This condition will be easy to satisfy for any c.g. location on a three-surface airplane.

This result could be inferred from Laitone's result for a two-surface airplane and by the simple application of Munk's theorem to the three-surface airplane. Since, in this case $g_{23}=0$ and $b_3=b_2$, the elliptically loaded third surface can be moved back to coincide with the elliptically loaded tail surface, giving a single surface with elliptical distribution of L_2+L_3. In this way, Laitone's result applies directly to a three-surface airplane having $g_{23}=0$ and $b_3=b_2$.

All Gaps Zero

If $g_{12}=g_{23}=g_{13}=0$, then $\sigma_{12}/(b_2/b_1)=\sigma_{23}/(b_3/b_2)=\sigma_{13}/(b_3/b_1)=1$ and Eq. (15) reduces to

$$\pi qD_i=\frac{W^2}{b_1^2}+\frac{(L_2+L_3)^2}{b_1^2}\left[\frac{b_1^2}{b_2^2}-1\right]+\frac{L_3^2}{b_1^2}\left[\frac{b_1^2}{b_3^2}-\frac{b_1^2}{b_2^2}\right] \tag{21}$$

In this case the "ideal minimum" drag can be obtained when $L_2=L_3=0$. The peanalty for loading the third surface when $L_2+L_3=0$ is proportional to $(b_1^2/b_3^2-b_1^2/b_2^2)$. This may be considered to arise from having a zero net load (nonelliptically distributed) when the two surfaces are moved longitudinally to coincide. The resulting single trim surface load distribution would then appear as shown in Fig. 7.

It may be noted also from Eq. (21) that since (b_1^2/b_2^2-1) may be less than $(b_1^2/b_3^2-b_1^2/b_2^2)$, circumstances may arise where it is better to hold $L_3=0$ and let L_2 vary from zero. If a given moment is to be produced, this method of trimming will produce lower induced drag when

$$\left(\frac{b_1^2}{b_3^2}-\frac{b_1^2}{b_2^2}\right)>\left(\frac{\ell_2-\ell_3}{\ell_2-\ell_1}\right)^2\left(\frac{b_1^2}{b_2^2}-1\right) \tag{22}$$

If $b_1/b_2=3$ and $(\ell_2-\ell_3)=3(\ell_2-\ell_1)$ this will occur when $b_2/b_3=3$.

If the trimming surface spans are made equal, Eq. (21) reduces to

$$\pi qD_i=\frac{W^2}{b_1^2}+\frac{(L_2+L_3)^2}{b_1^2}\left[\frac{b_1^2}{b_2^2}-1\right] \tag{23}$$

and the minimum induced drag occurs when $L_2+L_3=0$. The individual trim surface loads may have any magnitude as long as they are equal and of opposite sign. Under these conditions a trimming couple of any size and direction can be applied to a three-surface airplane without incurring an induced-drag penalty.

Table 3 compares this result with values taken from Table 2 for the two-surface configurations.

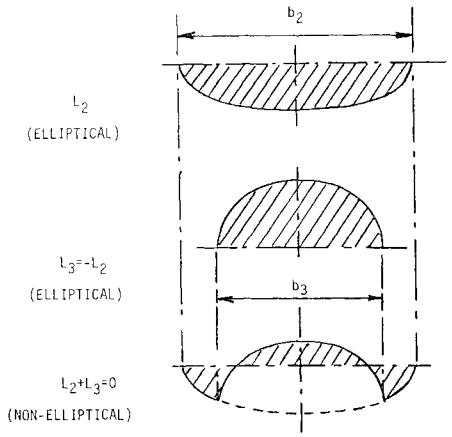

Fig. 7 Surface lift distributions.

Longitudinal Trim

For balance about the wing-body aerodynamic center,

$$M_1=M_0-W(\ell_1-\ell_w)-L_2(\ell_2-\ell_1)-L_3(\ell_3-\ell_1)=0 \tag{24}$$

and for minimum induced drag with zero gap and equal trimming surface spans, $L_3=-L_2$. Therefore, for longitudinal trim,

$$L_2(\ell_2-\ell_3)=M_0-W(\ell_1-\ell_w) \tag{25}$$

Equation (25) can be satisfied for any c.g. location ℓ_w by appropriate choice of L_2, and the minimum induced-drag condition will be met because $L_3=-L_2$.

Static Longitudinal Stability

From Eq. (6), the condition for positive static longitudinal stability of the three-surface airplane is found to be

$$\frac{\partial L_2}{\partial\alpha}(\ell_2-\ell_w)>\frac{\partial L_1}{\partial\alpha}(\ell_w-\ell_1)+\frac{\partial L_3}{\partial\alpha}(\ell_w-\ell_3) \tag{26}$$

In its dimensional form, the tail lift curve slope $\partial L_2/\partial\alpha$ includes the tail area S_2. Thus, any required static margin can be provided by appropriate choice of S_2 and ℓ_2.

Since it has already been shown that the minimum induced drag can be attained on a three-surface airplane with any c.g. location, and since surface loads do not appear explicitly in the static stability condition, there is no direct interaction between the minimum induced drag and stability conditions.

IV. Some Practical Considerations

The ideal theoretical results presented in the preceding sections indicate that the three-surface airplane can have a lower cruise trimmed drag than a conventional tail-aft design, which itself is superior to the pure canard configuration. However, an important consideration is whether these benefits are sustained under more practical circumstances. Some practical aspects are reviewed briefly below.

Nonelliptical Loading

Naylor[5] and Sachs[15] have shown that Prandtl-Munk estimates of induced drag due to trim for the conventional tail-aft design are not significantly affected by nonelliptical loading of the main wing. Naylor[5] finds good agreement with flight measurements, and Sachs[15] shows that the total interference drag is primarily a function of the average midsection wing downwash angle at downstream infinity and of the lift on the tail.

Feistal et al.[16] have shown by experiments on a canard-wing combination without a fuselage that the Prandtl-Munk theory overestimates the total induced drag by about 10% for that configuration. This finding has been explained and supported analytically by Butler[17] and Kroo.[18]

Rokhsaz and Selberg[19] have presented induced-drag estimates and wing spanwise lift distributions for their tri-wing design and indicate that the Prandtl-Munk theory underestimates the induced drag for the three-surface configuration.

All of these trends are explainable to a large extent by how closely the aggregate spanwise lift distribution of all of the lifting surfaces can approximate an elliptical form. In designs where no attempt is made toward this objective, the effects of nonelliptical loading on practical planforms then will be to compress the range of induced-drag differences between the three different configurations. For some applications the induced drag of inherently stable three-surface and conventional tail-aft designs may not be significantly different and the pure canard penalty may be reduced. This trend is indicated by Butler,[20] who includes a comparison of all three types over a

Table 3 Theoretical 'actual/ideal' induced-drag ratios

Configuration	c.g. location Aft	Fwd
1) Three-surface (No gaps, $L_2 = -L_3$, $b_3 = b_2$)	1.000	1.000
2) Conventional ($b_2/b_1 = 0.25$)	1.006	1.069
3) Canard ($b_3/b_1 = 0.50$)	1.229	1.316

range of static margins and lift coefficients. Some of these results have been summarized by this author in Ref. 21 which discusses this aspect more fully.

Profile Drag and Weight

Kroo[22] has produced comparisons of the relative drag of tail-aft, canard-wing, and three-surface designs. Lifting surface distributions are optimized for combinations of fixed total lift, trim with specified static margin, and fixed structural weight. Lift-dependent profile drag is included and the weight constraint ensures comparison on the basis of equal volume of material to support bending loads. No fuselage effects are included. General conclusions are that wing/aft-tail combinations achieve generally lower drag than wing-canard systems of equal weight and area. Three-surface configurations with small canard and tail surfaces do not experience the penalties associated with canard designs, but they may not always have a performance advantage over the conventional tail-aft type.

Fuselage Effects

The pressence of a fuselage is likely to have its maximum effect on the lift distribution on the forward surface of either the pure canard design or the three-surface design. This will then have a significant effect on the main wing lift distribution and on the total induced drag of the airplane. Consequently, comparisons between the three different configurations may change from that outlined above. Tests to investigate the effect of span ratio, stagger, and gap on a practical design have recently been made at Texas A&M with NASA support using a generic Learjet wind tunnel model. Results will be published in due course.

Potential Side Benefits

The apparent potential ability of the three-surface design to reduce trim drag has yet to be proven in practice. However, it seems probable that in applications where a large trimming moment is required, careful design of the three-surface design will produce performance benefits. Side benefits may accrue from a potential ability to relax wing section pitching-moment constraints that currently tend to limit the amount of advantage that can be taken from the supercritical airfoil technology. The ability of the three-surface design to reduce the trimming surface area required for some powered-lift arrangements has yet to be fully explored.

V. Conclusion

It has been shown that the three-surface airplane can attain minimum induced drag without compromising the conditions for longitudinal trim and static stability over a useful range of center-of-gravity (c.g.) locations. This is in favorable comparison with two-surface configurations for which longitudinal trim and minimum induced drag can be attained at only one c.g. location. A tail-aft design can have positive static stability at this c.g. location through the appropriate choice of tail volume. The pure canard is unstable at the minimum induced-drag c.g. location. For practical c.g. locations, the surface lift required for trim is more penalizing on the canard than on the tail-aft configuration.

Theoretical values of the actual/ideal induced-drag ratio for the different configurations studied in this paper are shown in Table 3.

It appears that the three-surface design can have better cruise efficiency in a stable trimmed condition over a practical range of c.g. locations than the conventional tail-aft design which, in turn, has much better cruise efficiency than the two-surface canard configuration.

These differences tend to be reduced when the nonelliptical loading on practical surfaces is included. Profile drag and surface weight considerations have a similar effect on the comparisons. Consequently, the advantages of the three-surface design over the conventional tail-aft design may be significant only for particular designs that are carefully designed to produce a higher-than-normal trim capability. Also, the increased drag increment of the pure canard designs predicted by the simple Prandtl-Munk theory may be approximately halved when practical effects are correctly accounted for.

Practical optimized designs of all three configurations should be studied further and tested to confirm these conclusions.

Acknowledgments

The author wishes to thank the management of Gates Learjet Corp. for permission to publish this paper. Also, a note of appreciation is due to Mrs. Marty Emmel for her typing.

References

[1]Prandtl, L., "Applications of Modern Hydrodynamics to Aeronautics," NACA Rept. 116, 1921.

[2]Prandtl, L., "Induced Drag of Multiplanes," NACA TN 182, 1924.

[3]Munk, M. M., "The Minimum Induced Drag of Aerofoils," NACA Rept. 121, 1921.

[4]Munk, M. M., "General Bi-Plane Theory," NACA Rept. 151, 1922.

[5]Naylor, C. H., "Notes on the Induced Drag of a Wing-Tail Combination," R&M 2528, 1954.

[6]Laitone, E. V., "Ideal Tail Load for Minimum Aircraft Drag," *Journal of Aircraft*, Vol. 15, March 1978, pp. 190-192.

[7]Laitone, E. V., "Positive Tail Loads for Minimum Induced Drag of Subsonic Aircraft," *Journal of Aircraft*, Vol. 15, Dec. 1978, pp. 837-842.

[8]Laitone, E. V., "Prandtl's Bi-Plane Theory Applied to Canard and Tandem Aircraft," *Journal of Aircraft*, Vol. 17, April 1980, pp. 233-237.

[9]Larrabee, E. E., "Trim Drag in the Light of Munk's Stagger Theorem," *Proceedings of the NASA-Industry-University General Aviation Drag Reduction Workshop*, Sess. V, Univ. of Kansas, Lawrence, July 1975.

[10]McLaughlin, M. D., "Calculations and Comparison with an Ideal Minimum of Trimmed Drag for Conventional and Canard Configurations Having Various Levels of Static Stability," NASA TN D-8391, May 1977.

[11]Keith, M. W. and Selberg, B. P., "Aerodynamic Optimization, Comparison, and Trim Design of Canard and Conventional High Performance General Aviation Configurations," AIAA Paper 83-0058, Jan. 1983.

[12]Laitone, E. V., "Reply by Author to R. S. Shevell," *Journal of Aircraft*, Vol. 15, Sept. 1978, p. 639.

[13]Shevell, R. S., "Comment on 'Ideal Tail Load for Minimum Aircraft Drag'," *Journal of Aircraft*, Vol. 15, Sept. 1978, p. 639.

[14]Durand, W. F., *Aerodynamic Theory*, Vol. V, Jan. 1943.

[15]Sachs, G., "Minimum Trimmed Drag and Optimum CG Position," *Journal of Aircraft*, Vol. 15, Aug. 1978, pp. 456-459.

[16]Feistal, T. W., Corsiglia, V. R., and Levin, D. B., "Wind Tunnel Measurements of Wing-Canard Interference and a Comparison with Various Theories," SAE Paper 810575, April 1981.
[17]Butler, G. E., "Effect of Downwash on the Induced Drag of Canard-Wing Combinations," *Journal of Aircraft*, Vol. 19, May 1982, pp. 410-411.
[18]Kroo, I. M., "Minimum Induced Drag of Canard Configurations," *Journal of Aircraft*, Vol. 19, Sept. 1982, pp. 792-794.
[19]Rokhsaz, K. and Selberg, B. P., "Analytical Study of Three-Surface Lifting Systems," SAE Paper 850866, April 1985.
[20]Butler, G. E., "An Analytical Study of the Induced Drag of Canard-Wing-Tail Aircraft Configurations with Various Levels of Stability," *The Aeronautical Journal of the Royal Aeronautical Society*, Oct. 1983.
[21]Kendall, E. R., "The Aerodynamics of Three-Surface Airplanes," AIAA Paper 84-2508, Oct. 1984.
[22]Kroo, I., "A General Approach to Multiple Lifting Surface Design and Analysis," AIAA Paper 84-2507, Oct. 1984.